

Evaluating the elastic properties of ensete fiber as a sustainable alternative to bast fibers: A micromechanical and numerical study

Barati Kelefatshe^a, Nonofa Emily Ramothokgwana^a, Mesfin Belayneh Ageze^b, Migbar Assefa Zeleke^{a*}

^aDepartment of Mechanical Engineering, University of Botswana, Gaborone 0061, Botswana

^bCenter for Renewable Energy Technology, College of Technology and Built Environment, Addis Ababa University, Botswana

ARTICLE INFO

Article history:

Received 28 August 2025

Accepted 30 November 2025

Available online

30 November 2025

Keywords:

Bast fibers

Ensete fiber

Natural fibers

Elastic properties

Micromechanics

Finite element method

ABSTRACT

Bast fibers are promising natural materials known for their biodegradability, affordability, and eco-friendliness, making them an alternative to synthetic options. Extensive research has been conducted to examine the effects of integrating various bast fiber reinforcements into epoxy and polystyrene matrices to boost the properties of the composite materials. However, there is limited research on ensete fiber and its utilization as a reinforcement that needs more in-depth research to be used as an alternative bast fiber. This paper aimed to predict and compare the performance of ensete fiber composites with six other bast fiber-reinforced polystyrene and epoxy composites. In this study, flax, hemp, jute, ramie, banana and kenaf were selected bast fibers for comparison purposes. This article employed various micromechanics models and finite element method (FEM), varying the fiber volume fraction. Our findings revealed that hemp fiber-reinforced composites exhibited the best predicted elastic properties, while banana fiber-reinforced composites showed the weakest performance. Notably, composites made with ensete fibers outperformed those made with jute and banana fibers in both epoxy and polystyrene matrices. Comparisons were made between results from the micromechanics models and FEM for all bast fiber-reinforced epoxy and polystyrene composites and there was an agreement between the effective elastic properties and fiber volume fraction (FVF). Further, bast-fiber reinforced epoxy composites showed higher values than polystyrene for strain analysis while for stress analysis, polystyrene composites showed higher stress loads than epoxy composites.

© 2026 Growing Science Ltd. All rights reserved.

Nomenclature

ANSYS	Analysis System	G_{12}	In-plane shear modulus of the composite
FEA	Finite Element Analysis	G_m	Shear modulus of the polymer matrix
MATLAB	Matrix Laboratory	G_f	Shear modulus of the fiber
RVE	Representative Volume Element	ν_m	Poisson's ratio for polymer matrix
FVF	Fiber Volume Fraction	ν_f	Poisson's ratio for natural fiber
V-R	Voigt-Reuss	ξ	Reinforcement factor
MD	Material Designer	η	Correction factor,
E_1	Longitudinal Young's modulus for the composite	ϕ_m	Maximum packing fraction
E_f	Young's modulus of the natural fiber	D_f	Fiber diameter in micrometers
V_f	Volume fraction of the natural fiber		
E_m	Young's modulus of the matrix		
V_m	Volume fraction of the polymer matrix		
E_2	Transverse Young's modulus for the composite.		

1. Introduction

Eco-friendly and biodegradable materials have been hailed as a superior alternative to making composite materials as a way of promoting sustainability, and in line with the increased awareness of renewable green resources (Gholampour & Ozbakkaloglu, 2020). The rise in global environmental concerns props green materials over and above synthetic resources.

* Corresponding author.

E-mail addresses: zelekem@ub.ac.bw (M. A. Zeleke)

ISSN 2291-8752 (Online) - ISSN 2291-8744 (Print)

© 2026 Growing Science Ltd. All rights reserved.

doi: 10.5267/j.esm.2025.11.004

Natural fibers present many advantages in comparison to synthetic fibers (Akil et al., 2011). Such advantages include, but are not limited to, biodegradability, low cost, and availability (Singh et al., 2023). Appealing characteristics like low cost, light weight, and high specific modulus prevalent in bast fibers have led many researchers to explore the use of bast fibers such as banana and jute as alternatives to synthetic fibers for reinforcing composite materials. (Kiruthika, 2017).

At present, natural fibers are available in a good number of developing countries, and they are currently making their way into various industries as they are used conventionally to produce ropes, yarns, mats, and paper, among others (Venkateshwaran & Elayaperumal, 2010). Mechanical and thermal characteristics of natural fiber-reinforced polymer composites are highly influenced by the fiber-matrix interface, and on the contrary, mechanical failures of these composites are mainly due to fiber pull-outs, fiber debonding, and breakage, which are all a result of poor adhesion to the matrix phase (Balaji et al., 2020). Shankar et al. (2013) also, reiterate that the mechanical properties of a natural fiber-reinforced polymer composite rely on the fiber modulus, strength, length, and orientation, besides the interfacial bond strength of the fiber and matrix.

Bast fibers provide a renewable, biodegradable, and cost-effective alternative to synthetic fibers as reinforcing material in composites (Mishra et al., 2022). However, even though they are environmentally friendly and cost-effective, there is not yet a fully comprehensive understanding of their mechanical properties, particularly the elastic properties of bast fibers themselves and bast fiber reinforced composites. Sustainability is a very important principle for many engineering applications today. Ensete fiber-reinforced composites are known to be biodegradable, have a low environmental impact and are cost-effective. There is however a limitation on their adoption due to limited data on their mechanical properties, especially their elastic behaviour. This lack of information is hindering the successful use of ensete fibers in a range of engineering applications such as the automotive industry, construction and aerospace engineering.

This paper is justified by the need to study and give a detailed and systematic comparison of bast fiber-reinforced composites. The paper will shed new light onto the limited data pertaining to the study of ensete fiber reinforced composites. The findings of this paper will fill a critical research gap offering great insights into the behaviour of these selected composites. The elastic properties under review for each composite are transverse and longitudinal Young's modulus, in-plane shear modulus and in-plane Poisson's ratio.

2. Materials

According to Dittenber & Gangarao (2012), bast fibers are collected from the stem. Both reinforcement fibers and matrix materials play vital roles in the composite. The reinforcement of bast fibers enhances the mechanical properties of the composite material (Bhowmik et al., 2021). This is because bast fibers possess superior physical and mechanical properties such as elevated modulus and specific strength, good process ability, low self-weight, low cost, and significant resistance to oxidization and fatigue (Gholampour & Ozbakkaloglu, 2020).

Contrary to their supernumerary advantages, natural bast fibers have several drawbacks such as limited compatibility with polymer resins, high moisture absorption and high anisotropy (Gholampour & Ozbakkaloglu, 2020). Problems arising from these disadvantages displayed by bast fibers can be cancelled by physical and chemical modification procedures on both the natural fiber and matrix (Arthanarieswaran et al., 2014). These procedures are mainly done to improve the mechanical properties of bast fibers so that they are more compatible with the matrix materials resulting in improved interfacial adhesion between the natural bast fiber and polymer matrix (Gholampour & Ozbakkaloglu, 2020).

A good interfacial bond is compulsory for optimal stress transfer from the matrix to the fiber through which maximum exploitation of the fiber strength in the composite is attained (Shankar et al., 2013). As such bast fibers are considered the best alternatives to be used as reinforcement in composites as compared to their synthetic counterparts. Due to the rapid decline in the supply of petroleum and its by-products and the increasing awareness on environmental problems arising from the use of artificial fibers because of their non-biodegradable nature, material scientists and engineers have been prompted to switch to natural bast fibers (Venkateshwaran & Elayaperumal, 2010; Yusuff et al., 2021).

Bast fibers commonly used include banana, jute, ramie, flax, hemp, kenaf and ensete (false banana) which are extracted from the skin and bast around the plants' stem (Gholampour & Ozbakkaloglu, 2020). The principal chemical properties within the average fibers are cellulose, hemicellulose, and lignin (Srinivas et al., 2024). As shown by **Table 1** below, each fiber under consideration has a varying weight percentage (wt. %) of the chemical properties.

These varying weight percentages of the chemical properties are mainly influenced by the different cultivation and harvesting conditions (Ari et al., 2023). When using weight considerations, cellulose constitutes a major portion of natural fibers (Teli & Terega, 2019) and it is an important structural element in natural fibers as it is a source of support and water retention in plant fibers (Srinivas et al., 2017). Lignin is also essential in plant fibers as it contributes towards the formation of cell walls (Srinivas et al., 2017). Other chemical properties of bast fibers which are present in less significant amounts include pectin, wax, and ashes (Srinivas et al., 2017).

Table 1. Chemical properties of natural fibers (Srinivas et al., 2024), (Teli & Terega, 2017)

Name of fiber	Cellulose (wt.%)	Hemicellulose (wt.%)	Lignin (wt.%)
Hemp	57-77	14-22.4	3.7-13
Flax	71	18.6-21.6	2.2
kenaf	45-77	8-13	21.5
Ramie	68.6-91	5-16.7	0.6-0.7
Jute	59-71.5	13.6-20.4	11.8-13
Banana	62-64	19	5
Ensete	64.46	22.47	6.88

Table 2 below displays the mechanical properties of the materials, both fibers and matrix phases used as inputs for the analysis.

Table 2. Mechanical Properties for different fibres and polymer matrices

Material	Young's modulus (GPa)	Poisson ratio	Shear modulus (GPa)	References
Epoxy	3.45	0.35	1.28	(Bhowmik et al., 2022) (Sudheer et al., 2015)
Polystyrene	3.4	0.33	1.278	(Bhowmik et al., 2022)
Banana	17.85	0.28	6.97	(Srinivas et al., 2024)
Ensete (False Banana)	26.7 ± 3 (Bekele et al., 2022)	0.175 (Batu & Lemu, 2021)	11.74	(Batu & Lemu, 2021; Bekele et al., 2022)
Flax	27.6	0.21	11.4	(Baley, 2002)
Hemp	70	0.4	25	(Bhowmik et al., 2022) (Anas Nisar & Jamil, 2023)
Jute	26.5	0.38	9.6	(V. Mariselvam and M. Logesh,)
Kenaf	53	0.32	20.1	(Srinivas et al., 2024)
Ramie	44	0.24	16.13	(Srinivas et al., 2024)

Ensete (False Banana)

Ensete (*Ensete Ventricosum*) is a plant which bears great potential for producing natural fibers (Batu & Lemu, 2021). Hailing from Ethiopia, the ensete plant is regarded as a sister to the banana plant owing to its closeness to the banana plant as depicted in **Fig. 1**. The ensete plant, scientifically known as *Ensete ventricosum* and part of the *Musa* family, is commonly referred to as the "false banana" because of its physical similarity to the banana plant (Temesgen et al., 2024). Ensete is cultivated as a staple food in Ethiopia with about 100 million plants harvested yearly for the provision of starchy food to 20% of the population (Dejene, 2024). This harvesting also results in the production of about 150k tons of ensete fiber. The major advantages of ensete fiber are its price and low density (Müller et al., 2017). The low density greatly contributes to ensete having superior strength to some other natural fibers (Dejene, 2024). False banana fiber-reinforced composites are a promising field of study due to their partial or complete biodegradability, widespread availability, low cost, and notable mechanical properties (Dejene, 2024).

Fig. 1 below illustrates Ensete plant and its fiber that is considered in this study.

**Fig. 1.** Ensete Plat and its Fiber (Borrell et al., 2020)

Banana

Bananas are large perennial plants whose parts cater for various needs such as fruits serving as a source of food, leaves as food wrapping and the stem as a source of fiber and paper pulp (Shankar et al., 2013). Banana plant is found in most Asian countries such as Thailand and Southeast Asian, India, Bangladesh, Indonesia, Malaysia, Philippines, Hawaii, and some Pacific islands (Verma et al., 2018). Approximately 70million metric tonnes of banana are produced annually in the world with India being the largest producer of banana at 27% share (Laxshaman Rao et al., 2021; Venkateshwaran & Elayaperumal, 2010b). In a review by Laxshaman Rao et al. (2021) it was indicated that for each hectare of banana cultivated, 220 tons of waste are produced which causes environmental problems such as the release of harmful greenhouse gases when dumped and burned. To deal with this waste, fiber is extracted from the biomass and can serve as a source of income for rural farmers (Prasad et al., 2016). Thus, banana fiber is a waste product of banana cultivation (Balaji et al., 2020b), meaning it's cheap and abundantly available for use (Sivaranjana & Arumugaprabu, 2021).

Being a ligno-cellulosic fiber, banana fiber is obtained from the pseudo stem of a banana plant and possesses good strength properties compared to conventional reinforcements such as glass (Verma et al., 2018). A banana plant has heights ranging from 3.0m to 12m (Verma et al., 2018). The fiber extracted from the banana plant is considered one of the strongest natural fibers with noted excellent durability (Adeniyi et al., 2021). In an evaluation article by (Arthanarieswaran et al. (2014), the banana fiber was shown to have beneficial physical properties with a Young's modulus of 3.5GPa and tensile strength of 56MPa. Prasad et al. (2016) highlighted other advantages of banana fiber such as good tensile strength, specific flexural strength, and rotting resistance. Due to its low density, high tensile strength and low elongation at break, banana fiber has been hailed as suitable for use in the construction automotive and machinery industries (Sivaranjana & Arumugaprabu, 2021). Sivaranjana & Arumugaprabu (2021) further goes on to prove that banana is a potential reinforcement in composite manufacturing as it is a suitable reinforcement in both thermoplastic and thermosets matrices due to its high strength and stiffness.

Hemp

Hemp is a fiber of interest in many industries spanning from agriculture to construction (Zimniewska, 2022). This plant has emerged to be one of the most widely used natural fibers as reinforcement in composites owing to their ecological friendliness (Shahzad, 2012). The fibers are strong and stiff since they are found in the stem to help keep the plant rigid. Hemp has desirable mechanical properties that make it useful as reinforcement for polymers. It is superior to other natural fibers due to its resistance to rot, durability, and high strength (Twite-Kabamba et al., 2009). The fibers also have high tensile strength. In a study by Dittenber & Gangarao (2012), hemp had a tensile strength of between 270 and 900 MPa. The strength significantly increases the load-bearing capacity of composites. This holds even in comparison to other composites using a different natural fiber such as jute. In a study done by Singh et al. (2023) where a hemp epoxy composite and jute epoxy composite were compared, the hemp-epoxy composite was found to have a greater strength and stiffness compared to the jute-epoxy composite.

Kenaf

In the *Malvaceae* plant family, there is a type of plant known as kenaf which is an allied fiber of the jute plant (Logesh M et al., 2017). The key producers of kenaf in the world are India, China and Thailand, accounting for 95% of the kenaf fiber produced in the world (Malik et al., 2021). Kenaf fiber can either be extracted from the bast, or the core resin of the plant. The fiber from the past possesses better mechanical strength (Bhambure et al., 2023). Tholibon et al. (2019) also mentions that the kenaf bast fiber exhibits good flexural strength and tensile strength when compared to the other kenaf fiber parts. Kenaf fiber is a good candidate for reinforcement in composites because it has high specific strength and modulus while also having low density, being non-abrasive and cost-effective (Bhambure et al., 2023). Also owing to their high cellulose content as shown in **Table 1**, kenaf fiber is one of the strongest existing natural fibers.

Ramie

Ramie is primarily cultivated in countries like China, Brazil, South Korea, the Philippines, Taiwan, Thailand, India, and several others China leads in production, contributing approximately 70% of the global supply, followed by Brazil and the Philippines. Ramie fiber is greatly used in the textile industry as it is one of the strongest natural fibers (Sriram & Sidhaarth, 2022). Ramie fiber is a kind of hemp fiber and due to its high cellulose content, high strength, and long fiber length, it has been considered an excellent material to be used as a reinforcement in polymer composites (Sun et al., 2011).

Ramie fiber has a tensile strength of between 400MPa and 1586MPa, having a higher tensile strength compared to other fibers such as flax and jute as shown in the 2020 analysis of Ramie Fiber and Woven Ramie Reinforced Epoxy Composite (Djafar et al., 2021). From this, it can be deduced that the use of ramie fiber as a reinforcer in composite materials can greatly improve the tensile strength of the composites. As analyzed by Paiva Júnior et al. (2004), composites that were reinforced by 45% of ramie fibers had an increase of up to 338% on their tensile strength when compared to bare polyester resin.

Jute

In recent years, jute has been growing in popularity due to an increase in environmental concerns and pollution (Shakir & Singh, 2024). According to Wang et al. (2019), jute is the second most natural and biodegradable fiber used in the world. As a flood-resistant crop, jute is easily cultivated in areas that receive high rainfall with 95% of jute cultivated in Asia (Shakir & Singh, 2024), (Ahamed et al., 2022). Jute grows well in tropical climates and has minimal impact on the environment (Gupta et al., 2024). Furthermore, jute has a disposable nature that is advantageous to the environment. Jute has notable advantages such as its abundance, low cost, and low density (Ahamed et al., 2022). In contrast, it also has disadvantages such as high energy consumption due to its intensive mechanical steps in the manufacturing process (Ahamed et al., 2022). Jute is one of the most manufactured fibers in the world and has applications in many industries such as textile, transportation, and even some load-bearing applications. It is a common and effective reinforcement for composites (Gupta et al., 2024). These include but are not limited to household, engineering, building structures, door frames, shopping bags, and furniture (Prasanthi et al., 2022). Azim et al. (2022) has noted that the demand for jute has risen owing to its use in structural composites.

Flax

One of the oldest textile fibres known to humans is the flax fiber. It has served as the basis for many productions such as the fabric, clothing, sails and tents industries (Bos, 2004). Approximately 5 million hectares of flax is cultivated in the world with most of it being in Canada, USA, Russia and Europe (Bos, 2004). Flax has one of the shortest growth cycles with just 100 days between sowing and harvesting each in March and July respectively (Yan et al., 2014). Flax fiber has been shown to be an excellent choice for composites with extensive mechanical properties while being environmentally friendly and economical. The other advantage of flax fiber is that it offers the intersection of low cost, light weight and high strength and stiffness (Dittenber & Gangarao, 2012). For an option of a low-density, easy-to-handle, eco-friendly and easily available type of fiber, the flax fiber is the best choice (Malik et al., 2022).

Flax fiber is a cost-effective material with the potential to replace glass fibers as reinforcement. The use of flax can be attributed to its ease of production and its outstanding mechanical properties (Romhányi et al., 2003). At just a length of 80cm plant, the flax fiber has a mean strength of 1200MPa and a mean young modulus of 60GPa (Charlet et al., 2009). The fibers are found at the periphery of the stem cross-section, and they are strong. Flax is eco-friendly and provides biodiversity through the rotation of crops. There is still greater variability in the mechanical properties of flax fibers. These are influenced by field conditions and potential damage in the production processes (Yan et al., 2014).

The main disadvantage of natural fibers is poor compatibility between fiber and matrix as natural fibers tend to be hydrophilic, leading to high moisture absorption. Ensete being a classification of natural fibers also presents such drawbacks. To remedy this, ensete fibers are chemically treated to modify their fiber surface and improve their strength, which leads to low water/moisture absorption and overall improvement in mechanical properties (Ketema & Dar, 2021). In a study by Teli & Terega (2019) ensete fibers displayed great improvement in thermal stability, tenacity, tensile and structural properties after being treated with 10% sodium hydroxide (NaOH). In another study on the "Optimization of ethanol-alkali delignification of false banana (*Ensete ventricosum*) fibers for pulp production using response surface methodology" ensete fibers were delignified to produce high-yield resistant pulps by using sulphur-free ethanol-alkali pulping (Berhanu et al., 2018). Dunisho et al. (2020) goes on to further say alkali treatment is not just effective in cleaning the fiber surface by the removal of impurities, it also gives the fiber a coarser surface thus improving the adhesion or interface between the fiber itself and the matrix in the formation of composites.

3. Micromechanics Models

This study partly utilizes analytical models to predict the elastic properties of materials through mathematical expressions. These models are divided into two main categories: micromechanical models and semi-empirical models. Micromechanical models are designed to estimate the bulk properties of materials by analyzing their microstructures. They predict the overall behavior of composites based on the characteristics of their constituents, specifically the fibers and the matrix. On the other hand, semi-empirical models blend theoretical predictions with experimental data to assess the overall properties of composites. In this study, we will employ several commonly used models, including the Halpin-Tsai, Rule of Mixture (ROM), Nielsen Elastic, and Chamis models (Sudheer et al. 2015).

Rule of Mixture Model

A key task in the mechanics of materials is predicting how materials behave, which involves estimating their effective properties through the process of homogenization. One of the simplest methods for achieving homogenized properties in heterogeneous materials is the rule of mixtures (ROM) (Sudheer et al. 2015) where the overall properties are calculated as an average of the individual constituents' characteristics. This model assumes that fibers are evenly distributed, the polymer matrix is free of voids, and there is a perfect bond between the fibers and the matrix (Bhowmik et al. 2021). The following equations will be employed to estimate the elastic properties of composites using this model (Sudheer et al. 2015, Bhowmik et al. 2022).

$$E_{(c,L)} = E_f V_f + E_m V_m = E_1 \quad (1)$$

where: E_1 represents the composite's longitudinal Young's modulus, E_f and V_f are the Young's modulus and volume fraction of the natural fiber respectively and E_m and V_m represent Young's modulus and volume fraction (VF) of the matrix respectively. The following equation was employed to predict the transverse modulus.

$$E_{(c,T)} = \frac{E_m E_f}{E_m V_f + E_f V_m} = E_2 \quad (2)$$

where: E_2 is the transverse Young's modulus for the composite. The in-plane shear modulus was computed using the following equation (Bhowmik et al., 2022),

$$G_{12} = \frac{G_f G_m}{G_m V_f + G_f V_m} \quad (3)$$

where G_{12} is the in-plane shear modulus of the composite, G_m and V_m represent the shear modulus and volume fraction of the polymer matrix respectively and G_f and V_f are the shear modulus and VF of the fiber respectively.

The Poisson ratio was calculated using Eq. (4) (Bhowmik et al., 2022; Sudheer et al., 2015).

$$v_c = v_m V_m + v_f V_f \quad (4)$$

where v_f and v_m represent Poisson's ratio for natural fiber and polymer matrix respectively

Halpin-Tsai Model

The Halpin-Tsai model is a well-known and primary semi-empirical model for computing transverse elastic properties of composites (Zhou et al. 2024). This model involves chains of empirical procedures to designate the reinforcing performance of composites by considering correcting factors. From this model, the transverse Young's modulus of the composite can be computed as detailed in Eq. (5) (Yun et al. 2022).

$$E_{(c,T)} = E_m \left(\frac{1 + \eta \xi V_f}{1 - \eta V_f} \right) \quad (5)$$

In Eq. (5), ξ signifies reinforcement factor and has a value of 2 for a square packing of circular fiber. Further the correction factor η is given as follows (Bhowmik et al. 2021, Yun et al. 2022).

$$\eta = \frac{\left(\frac{E_f}{E_m} - 1 \right)}{\left(\frac{E_f}{E_m} + \xi \right)} \quad (6)$$

Eq. (7) below gives the shear property (Yun et al. 2022)

$$G_c = G_m \left(\frac{1 + \eta \xi V_f}{1 - \eta V_f} \right) \quad (7)$$

Neilsen Elastic Model

This model actually modifies the Halpin-Tsai model by incorporating the maximum packing fraction (φ_m) (Bhowmik et al. 2021) which is influenced by the geometric configuration of the composite materials (Sudheer et al. 2015). The following equation was used to calculate the transverse modulus of the composite (Sudheer et al. 2015, Bhowmik et al. 2022).

Nelsen's model basically adapts Halpin Tsai's model by including the maximum packing fraction (φ_m) (Bhowmik et al. 2022). The shear and transverse modulus can be computed respectively as follows.

$$G_c = G_m \left(\frac{1 + \eta \xi V_f}{1 - \omega \eta V_f} \right) \quad (8)$$

$$E_{(c,T)} = E_m \left(\frac{1 + \eta \xi V_f}{1 - \omega \eta V_f} \right) \quad (9)$$

and ω was calculated using the equation (Sudheer et al. 2015, Bhowmik et al. 2022),

$$\omega = 1 + \frac{1-\varphi_m}{\varphi_m^2} V_f \quad (10)$$

Chamis Model

The Chamis model is a modified version of the rule of mixtures that substitutes the FVF with square root of FVF (Sudheer et al. 2015, Younes et al. 2012). This model is widely used and reliable semi empirical techniques in the prediction of elastic properties. The longitudinal and transversal properties can respectively be computed as follows (Sudheer et al. 2015, Yun et al. 2022, Younes et al. 2012).

$$E_{(c,L)} = E_f V_f + E_m V_m \quad (11)$$

$$E_{(c,T)} = \frac{E_m}{1 - \left\{ \sqrt{V_f} \left(1 - \frac{E_m}{E_f} \right) \right\}} \quad (12)$$

Further the Poisson's ration can be calculated as below (Sudheer et al. 2015, Yun et al. 2022, Younes et al. 2012).

$$v_c = v_m V_m + v_f V_f \quad (13)$$

The longitudinal and transversal shear properties can also be computed respectively as follows (Sudheer et al. 2015, Yun et al. 2022, Younes et al. 2012).

$$G_{(c,L)} = \frac{G_m}{1 - \left\{ \sqrt{V_f} \left(1 - \frac{G_m}{G_{f,L}} \right) \right\}} \quad (14)$$

$$G_{(c,T)} = \frac{G_m}{1 - \left\{ \sqrt{V_f} \left(1 - \frac{G_m}{G_{(f,T)}} \right) \right\}} \quad (15)$$

4. Finite Element Method (FEM)

Experimental test is without a doubt the leading approach to substantiate the perdition of mechanical properties of a composite. However, sample preparation and testing materials are time intensive, costly, and error prone. Hence, FEM is a feasible numerical approach to deal with the above limitations. FEM is one of the most common numerical techniques that has been widely used by scholars to calculate the elastic properties of composites. In this study, polystyrene and epoxy have been used as a matrix of ensete-fiber reinforced composites. Here it is assumed that the matrix and fiber are homogeneous and isotropic. A 3D representative volume element (RVE) with a square packing and circular cross-section of ensete fiber has been developed as shown in **Fig. 2**. The RVE is effectively sized to reasonably symbolize the composite statistically (Adeniyi et al. 2021).

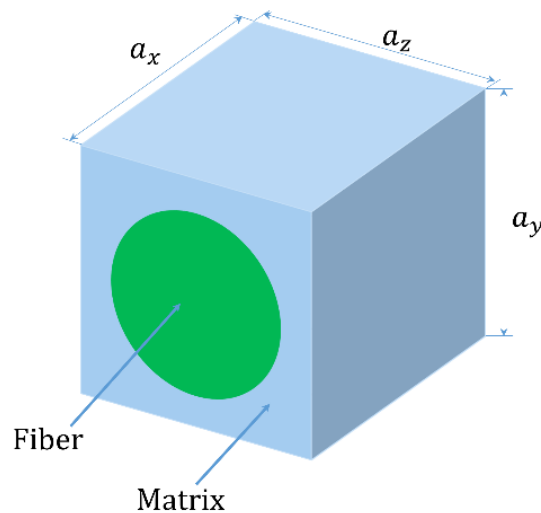


Fig. 2. Square RVE with a circular Ensete fiber

For analysis purposes, the dimensions of the RVE were taken as $a_x = a_y = a_z = 1.2 \times 10^{-3} m$ (Adeniyi et al. 2021). The fiber diameter of the RVE and the fiber volume fraction were related by the following equation which was used to determine the fiber diameter at the varying fiber volume fractions. The equation below shows the relation between the FVF and the fiber diameter.

$$D_f = \sqrt{\frac{4LWV_f}{\pi N}} \quad (16)$$

where: D_f is the fiber diameter in micrometers, W and L are the RVE width and length respectively, and N is the number of fibers in the composite. The radius of the fibers directly corresponds to the FVFs. This study evaluated the elastic properties of the composites across a FVFs range of 0 to 1. Composites can be classified as orthotropic, anisotropic, or transversely isotropic (Agwu et al. 2022). For anisotropic materials, whose properties vary in all directions, the following constitutive equation applies (Adeniyi et al. 2021).

$$\sigma = C\varepsilon \quad (17)$$

where σ , ε and C represent the stress vector, strain vector, and stiffness matrix, respectively. When transformed into three dimensions, the equation becomes:

$$\begin{Bmatrix} \sigma_1 \\ \sigma_2 \\ \sigma_3 \\ \sigma_4 \\ \sigma_5 \\ \sigma_6 \end{Bmatrix} \equiv \begin{Bmatrix} \sigma_{xy} \\ \sigma_{yy} \\ \sigma_{zz} \\ \sigma_{yz} \\ \sigma_{zx} \\ \sigma_{xy} \end{Bmatrix} = \begin{bmatrix} C_{11} & C_{12} & C_{13} & C_{14} & C_{15} & C_{16} \\ C_{12} & C_{22} & C_{23} & C_{24} & C_{25} & C_{26} \\ C_{13} & C_{23} & C_{33} & C_{34} & C_{35} & C_{36} \\ C_{14} & C_{24} & C_{34} & C_{44} & C_{45} & C_{46} \\ C_{15} & C_{25} & C_{35} & C_{45} & C_{55} & C_{56} \\ C_{16} & C_{26} & C_{36} & C_{46} & C_{56} & C_{66} \end{bmatrix} \begin{Bmatrix} \varepsilon_{xy} \\ \varepsilon_{yy} \\ \varepsilon_{zz} \\ \varepsilon_{yz} \\ \varepsilon_{zx} \\ \varepsilon_{xy} \end{Bmatrix} \equiv \begin{Bmatrix} \varepsilon_1 \\ \varepsilon_2 \\ \varepsilon_3 \\ \varepsilon_4 \\ \varepsilon_5 \\ \varepsilon_6 \end{Bmatrix} \quad (18)$$

This study considers the transversely isotropic characteristics of ensete fiber-reinforced polystyrene and epoxy composites. Transversely isotropic material has a single axis of symmetry and exhibits isotropic properties in one of the planes (Adeniyi et al. 2021). Since this study focuses on transversely isotropic materials (Adeniyi et al. 2021, Agwu et al. 2022), the above 3-D constitutive equation simplifies the following form.

$$\begin{Bmatrix} \sigma_1 \\ \sigma_2 \\ \sigma_3 \\ \sigma_4 \\ \sigma_5 \\ \sigma_6 \end{Bmatrix} = \begin{bmatrix} C_{11} & C_{12} & C_{13} & 0 & 0 & 0 \\ C_{12} & C_{22} & C_{23} & 0 & 0 & 0 \\ C_{13} & C_{23} & C_{33} & 0 & 0 & 0 \\ C_{14} & C_{24} & C_{34} & \frac{1}{2}(C_{22} - C_{23}) & 0 & 0 \\ C_{15} & C_{25} & C_{35} & 0 & C_{66} & 0 \\ C_{16} & C_{26} & C_{36} & 0 & 0 & C_{66} \end{bmatrix} \times \begin{Bmatrix} \varepsilon_1 \\ \varepsilon_2 \\ \varepsilon_3 \\ \varepsilon_4 \\ \varepsilon_5 \\ \varepsilon_6 \end{Bmatrix} \quad (19)$$

The axis of symmetry is assumed to be aligned with the fiber direction (Agwu et al. 2022). For the homogenized material, the elastic properties can be determined using the following equations, provided the values of the transversely isotropic stiffness matrix 'C' are known.

$$E_1 = C_{11} - \frac{2C_{12}^2}{C_{22} + C_{23}} \quad (20)$$

$$E_2 = \frac{[C_{11}(C_{22} + C_{23}) - 2C_{12}^2](C_{22} - C_{23})}{(C_{11}C_{22} - C_{12}^2)} \quad (21)$$

$$v_{12} = \frac{C_{12}}{C_{22} + C_{23}} \quad (22)$$

$$G_{23} = \frac{1}{2}(C_{22} - C_{23}) \quad (23)$$

where: E_1 and E_2 represent the longitudinal and transverse modulus respectively, G_{23} and v_{12} denote an in-plane shear modulus and in-plane Poisson's ratio respectively (Adeniyi et al. 2021). ANSYS Material Designer (MD) was employed for the Finite Element Analysis (FEA) of ensete fiber-reinforced polymer composites. MD is a built-in tool in ANSYS Workbench that facilitates modeling and analysis. Its advantages include a variety of pre-defined fiber-reinforced geometries, which streamline the creation of Representative Volume Element (RVE) models for fiber-reinforced composites, saving time. Instead of analyzing the entire macroscopic composite, we use an RVE for material characterization, applying periodic boundary conditions. This simplified RVE incorporates both fiber and matrix materials. **Fig. 3** shows the square arrangement available in ANSYS for unidirectional composite materials. In this study, a mesh size of 0.1 μm was applied to the RVE. Tetrahedral elements were used, resulting in a total of 1,464 elements and 2,196.

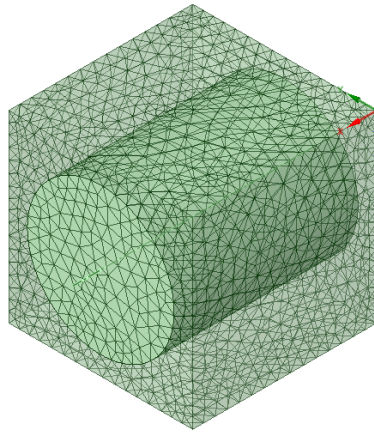


Fig. 3. ANSYS generated RVE with single fibre

5. Results and Discussions

5.1 Results from Micromechanics Models

5.1.1 Axial modulus (E_1) results for all fibers using Rule of Mixture

Fig. 4 shows the axial modulus (E_1) values from micromechanics models across various fiber volume fractions. On the left labelled a) are the epoxy values and on the right labelled b) are polystyrene composites. The effective axial modulus (E_1) varies between the two composite types. Noticeably though for both types of composites the graphs have the same structure with an increase of E_1 with increase in FVF. This is observed from ROM micromechanics model. The conclusion from this is that there is a strong relationship between fiber content and stiffness in a composite. This stiffness supports the idea of using bast fiber as reinforcement in composites. The higher the fiber content the more axial load bearing the composite has.

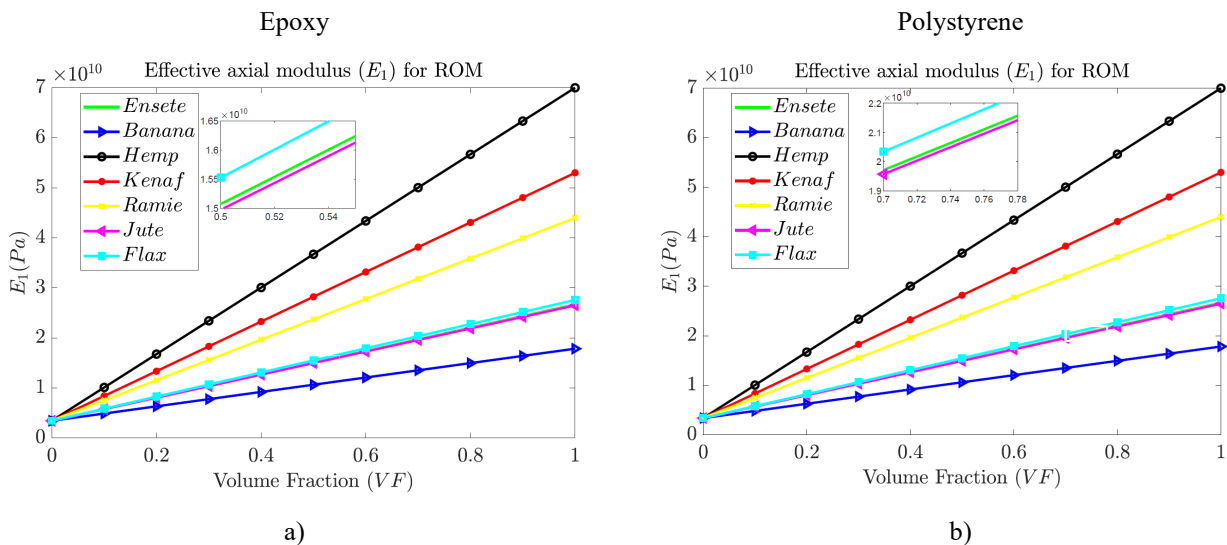


Fig. 4: E_1 -ROM values for a) epoxy composites and b) polystyrene composites

In epoxy, Hemp fiber composites consistently yield the highest of E_1 values than all the other fibers whereas banana fiber composites yield the lowest of E_1 values. For hemp epoxy polystyrene in Rule of Mixture, Halpin Tsai and Chamis, the axial modulus is at 36.73GPa at 0.5 fiber volume fraction which is the highest recorded. Likewise, the banana epoxy composite consistently records 10.65 GPa at 0.5 fiber volume fraction, the lowest for all epoxy composites. The other fiber epoxy composites range between the two values, for example flax, jute and kenaf are around 15.5GPa and kenaf at 28.23GPa. Hemp polystyrene composites have the highest axial modulus compared to other fiber polystyrene composites. In **Fig. 4 b)**, E_1 for hemp polystyrene composites are at 36.7GPa while others are trailing below it. Just like the banana-epoxy composite, the banana-polystyrene composites have the lowest of E_1 values across all models compared to other fibers. The trend seen of hemp composites having the highest of all axial modulus values suggests that hemp fibers contribute greater stiffness in the axial direction while banana contributes the lowest and ramie, jute, kenaf, flax and ensete are ranging in between. In all the models the graphs appear relatively straight across fiber types and matrix materials, which suggests that within the tested

range, the fiber-matrix interaction maintains a consistent impact on axial stiffness across these composites and suggests that there is a stable fiber matrix interaction in the tested range.

5.1.2 Transversal modulus (E_2) results for all fibers using the Rule of Mixtures

The graphs of transverse Modulus (E_2) are seen from **Fig. 5**. In contrast with E_1 , E_2 exhibits a non-linear relationship with VVF. There is an increased complexity of stress distribution in the transverse direction in composites, hence the observed trend. True still to the observations of E_1 , epoxy-hemp composites show a higher E_2 than other fiber composites, reinforcing the observation that hemp has superior mechanical properties in both axial and transverse directions. In **Fig. 5 (a)**, at 0.5 fiber volume fraction hemp has $E_2 = 6.58$ GPa while other fiber epoxy composites have less than that and banana epoxy composite has the lowest at $E_2 = 5.78$ GPa. The Chamis model outputs a larger value of E_2 for fiber-epoxy composites compared to the other models. E_2 obtained from Chamis model is 10.53 GPa for hemp at 0.5 fiber volume fraction compared to 6.58 GPa and 5.96 GPa in the Rule of Mixture and Nielsen models respectively. The same is observed for the remaining fibers like ensete which has 10.11 GPa, 6.11 GPa and 5.34 GPa for Chamis, Rule of mixture and Halpin Tsai respectively. For the polystyrene composites, hemp still has the highest value of E_2 . Banana has the lowest and kenaf, ensete, flax and jute are still in between the two.

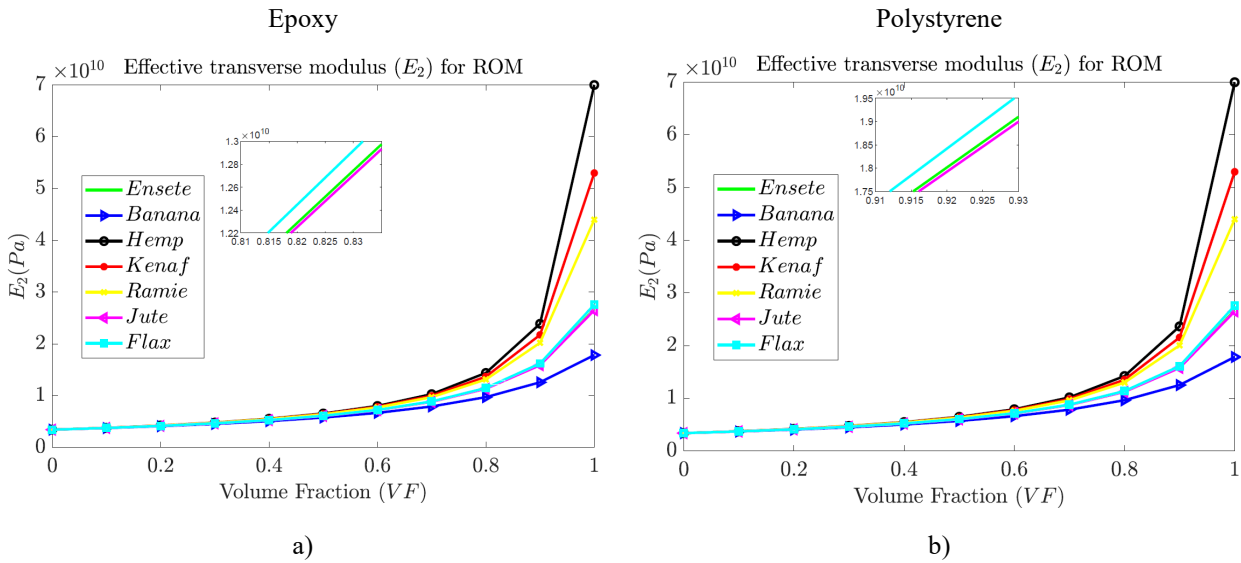


Fig. 5. E_2 -ROM results for a) epoxy composites and b) polystyrene composites.

5.1.3 Shear modulus (G_{12}) results for all fibers using the Rule of Mixtures

The shear modulus (G_{12}) values are observed from **Fig. 6** for both epoxy and polystyrene composites.

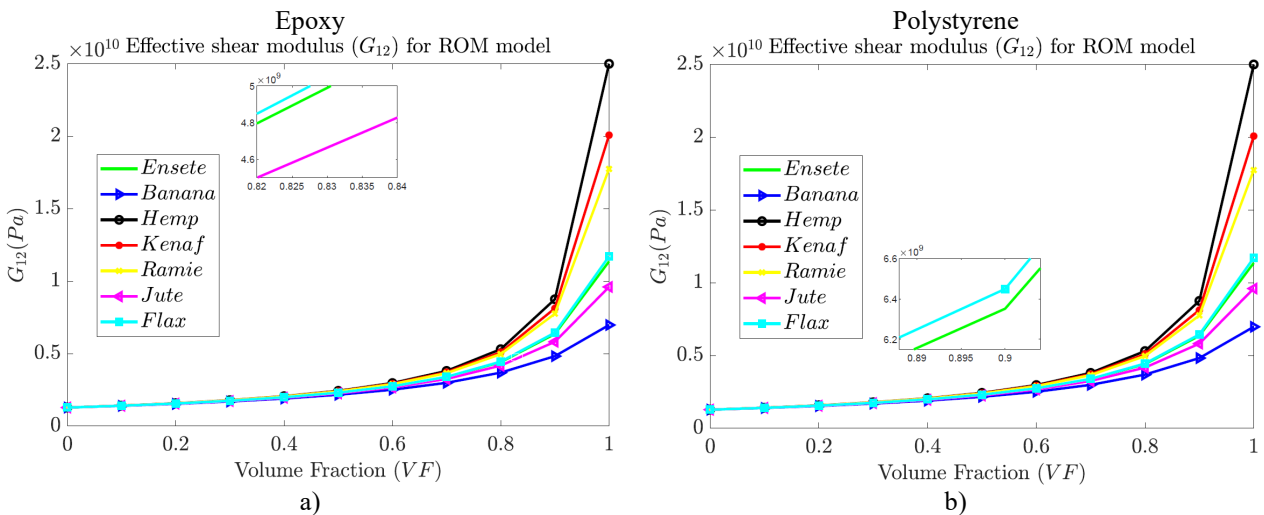


Fig. 6. G_{12} -ROM results for a) epoxy composites and b) polystyrene composites.

For shear modulus (G_{12}), a pattern is observed where hemp composites exhibit higher G_{12} values than other composites. But unlike with E_1 and E_2 the difference is not as significant at lower fiber volume fractions. In the epoxy composite, using Rule of Mixture at 0.5 FVF values of G_{12} range between 2.16 GPa (banana) and 2.43 GPa (hemp). Likewise, the polystyrene composites range around the same values. The Rule of Mixtures and Chamis models yield a bit lower estimate of G_{12} , while

the Halpin-Tsai and Nielsen models present higher values, especially at greater fiber volume fractions beyond 0.5. This difference indicates that these models account differently for fiber-matrix interfacial bonding strength under shear loading, and as expected the more complex models (Halpin Tsai and Nielsen) potentially better captures the mechanics involved in the composites and ultimately the resulting properties. The increase in G_{12} with fiber volume fraction demonstrates that fibers effectively resist shear deformation, albeit to a lesser extent than axial stresses.

5.1.4 Poisson's ratio (ν_{12}) results for all fibers using the Rule of Mixtures

Fig. 7 demonstrates how the Poisson ratio ν_{12} varies with increasing fiber volume fractions. Graphs with a positive gradient are observed for fibers with Poisson ratio higher than that of the matrix used and vice versa. For all the graphs, hemp and jute have an increasing Poisson ratio with an increase in fiber volume fraction whereas the rest of the fibers are the opposite. The other remaining fibers have a Poisson ratio below the values for epoxy and polystyrene. The Poisson ratio is largely governed by matrix properties, which explains the relatively small variation across composites and fiber types. On the matrix themselves, epoxy, being a stiffer matrix, results in slightly lower ν_{12} values than polystyrene, which allows more lateral deformation. Despite these minor changes, the consistency across models highlights that the fiber-matrix interaction influences lateral strain to a lesser extent than axial or shear properties.

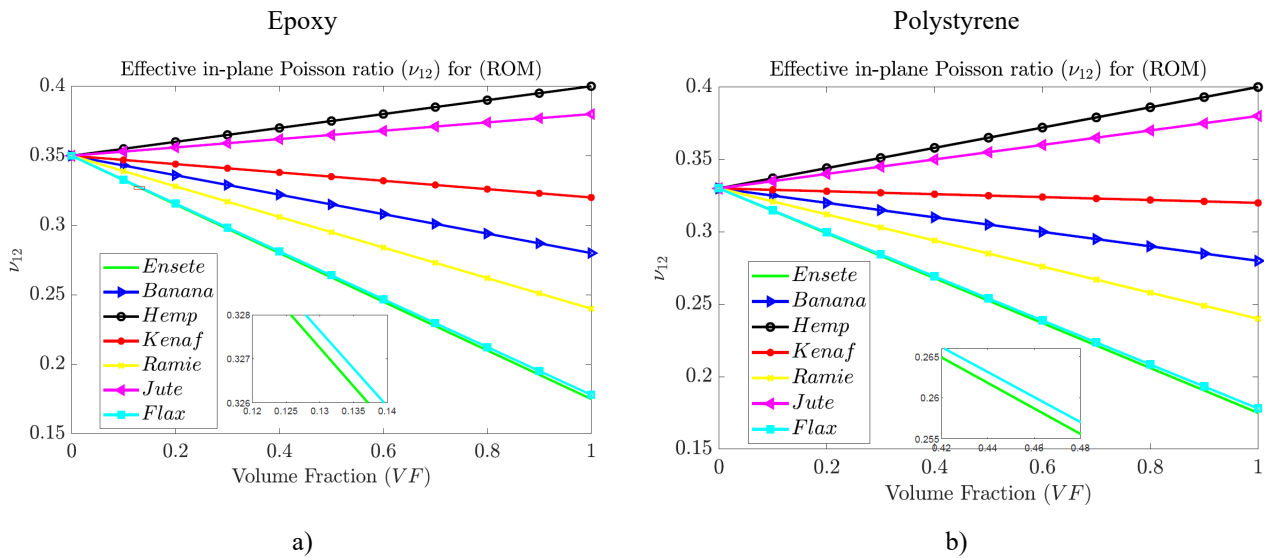


Fig. 7. ν_{12} -ROM results for a) epoxy composites and b) polystyrene composites.

As evident by **Fig. 4** through to **Fig. 7** among the fibers, hemp has superior characteristics in either matrix for all the models used for evaluation. This is because it has a high modulus that indicates greater stiffness, which improves the bearing capacity of the composite. Hemp's rigid structure, reflected in its elastic modulus, facilitates efficient stress transfer within the matrices. The values of the fibers in both matrix, evaluated through the elastic properties and models used, did not vary greatly. Even though that is true, epoxy-based composites have superior characteristics. Examples can be seen using different fibers and models. Although the examples stated are isolated and few, the statement holds true for all the fibers, the fiber volume fractions and the models. E_1 Values of 0.5 banana fiber volume fraction are 10.65GPa in epoxy and 10.63GPa in polystyrene, both using Rule of Mixture **Fig. 4**. E_2 Values for 0.5 hemp volume fraction in epoxy are 10.53GPa in epoxy and 10.39 in polystyrene using the Chamis model. G_{12} values of 0.5 kenaf volume fraction are 4.00GPa in epoxy and 3.78 in polystyrene using the Halpin Tsai model. For 0.5 flax volume fraction in epoxy, the ν_{12} value is 0.264 whereas it is 0.254 for polystyrene in the Chamis model. Epoxy is a thermoset, and it generally has a stiffer matrix and better mechanical properties as evident by **Table 2** which is the main reason why it performs better as a matrix.

There is an increase in E_1 , E_2 and G_{12} values of the composite when switching from using polystyrene to an epoxy matrix. The opposite occurs in the reverse direction. Examples are the use of polystyrene with a kenaf matrix which yields an E_1 of 28.2 but 28.23 when used with epoxy resulting in a 0.10% increase at 0.5 volume fraction. The use of bananas in a polystyrene matrix yields an E_2 of 5.71 GPa whereas in epoxy it is at 5.78 GPa at 0.5 fiber volume fraction. There is a 1.23% increase due to the switch from polystyrene to epoxy. As observed in ensete values for both epoxy and polystyrene are 3.45 GPa for G_{12} meaning there is a 0% increase.

5.2 Comparative study on Ensete fiber composites

5.2.1 Axial modulus (E_1) results for Ensete composites

Fig. 8 shows the effect of increasing the FVF on the longitudinal modulus for both ensete fiber-reinforced epoxy composite (EFREC) and ensete fiber-reinforced polystyrene composite (EFRPC) using all micromechanical models and FEA. From the

plot, it is observed that there is a linear relationship between the effective longitudinal modulus and the ensete FVF. The predicted values for the longitudinal modulus for the EFREC and EFRPC are found to be 15.11GPa and 15.08GPa respectively for a fiber volume fraction of 50%. It is also noticed that all results from models of micromechanics and FEA align for both composites as they all conform to the Rule of Mixtures values. This validates the results from the micromechanical models and proves the results to be much more accurate and reliable.

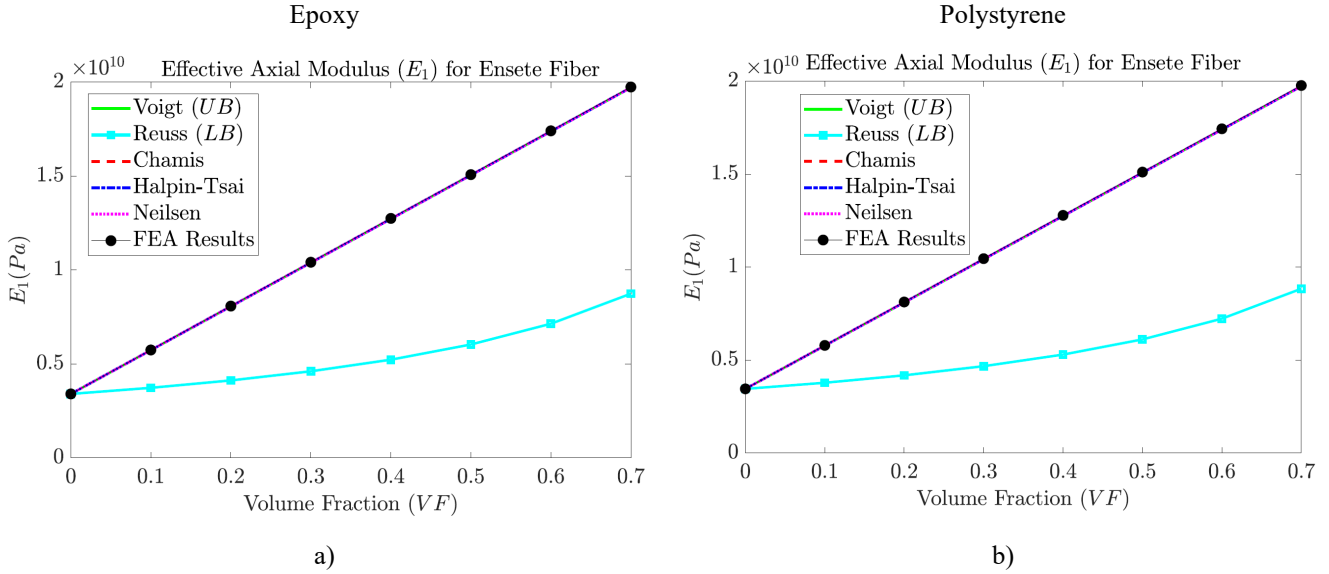


Fig. 8. E_1 -FEA and micromechanical models' result comparison for a) ensete/epoxy composite and b) ensete/polystyrene composite.

5.2.2 Transverse modulus (E_2) results for Ensete composites

Fig. 9 (a-b) shows the equivalent transverse modulus of the ensete fiber-reinforced epoxy and EFRPC.

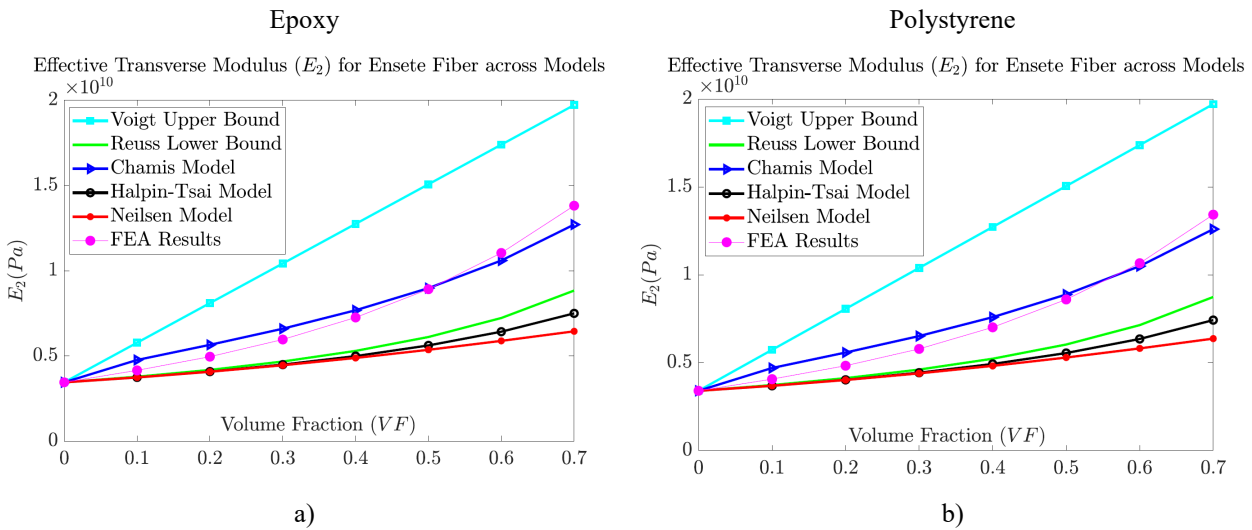


Fig. 9: E_2 -FEA and micromechanical models' result comparison for a) ensete/epoxy composite and b) ensete/polystyrene composite.

Although not directly proportional as with the longitudinal modulus, an increase in the effective transverse modulus with an increase in fiber volume fraction is observed for both the ensete fiber-reinforced composite and the EFRPC. At 0.5 FVF, the predicted effective in-plane transverse modulus is found to be 8.88 GPa for ensete fiber-reinforced polystyrene from Chamis model and 8.6 GPa for FEA, while for the ensete fiber-reinforced composite the corresponding E_2 value to 50% fiber volume fraction is found to be 8.91 GPa for both Chamis and FEA. This proves again that the EFREC exhibits better elastic properties as compared to the EFRPC. From these results, it can be deduced that the E_2 results from the Chamis model and FEA are in correlation, validating the robustness of the Chamis model, considering also that they fall within the Voigt upper and Reuss lower bounds of the elastic modulus as compared to the Halpin-Tsai and the Neilsen models, which are seen to deviate from the V-R bounds of the elastic modulus and also yielded the lowest values of the in-plane transverse modulus both composites.

5.2.3 Shear modulus (G_{12}) results for Ensete composites

Variation of the shear modulus with fiber volume fraction is displayed in **Fig. 10**. Results from all the analytical models all depict a non-linear increase of in-plane shear modulus for both EFREC and EFRPC. Again, using a FVF of 0.5 for comparison, of all the analytical models, Halpin-Tsai and Chamis models yielded a higher in-plane shear modulus than the FEM and Nielsen model for ensete fiber-reinforced epoxy composite. The same observation is made for the EFRPC. These results have a small deviation from the FEA results for both composites. For the EFRPC, the shear modulus predictions obtained from FEA were reduced by 13% from those predicted by the Chamis and Halpin-Tsai models giving a predicted value of 3.00GPa which was also predicted by the Nielsen model. Given the small deviation and the alignment with the Nielsen model results, it can be concluded that the predicted results obtained from both the micromechanical models and FEA are valid. As for the ensete fiber-reinforced epoxy composite, the predicted FEA and Nielsen model values for in-plane shear modulus were reduced by 13% compared to the Chamis and Halpin-Tsai predicted value for 0.5 fiber volume fraction. Considering that these values have a smaller deviation, and they also fall within the Voigt and Reuss bounds, the robustness of the modelling techniques is validated.

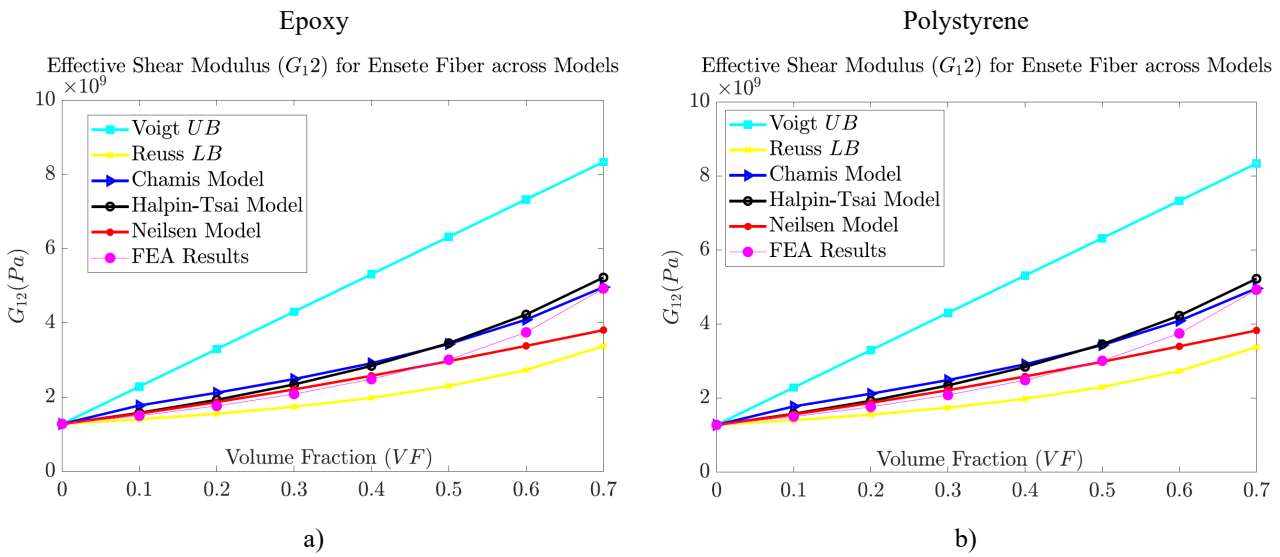


Fig. 10: G_{12} -FEA and micromechanical models’ result comparison for a) ensete/epoxy composite and b) ensete/polystyrene composite.

5.2.4 Poisson ratio (ν_{12}) results for Ensete composites

Fig. 11 displays the variation of in-plane Poisson’s ratio with FVF.

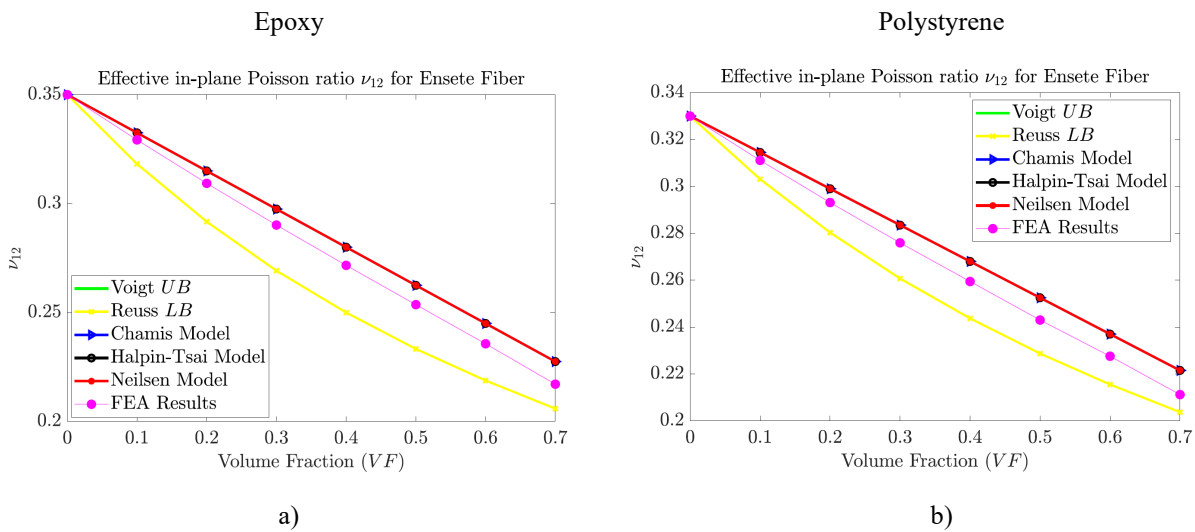


Fig. 11: ν_{12} -FEA and micromechanical models’ result comparison for a) ensete/epoxy composite and b) ensete/polystyrene composite.

For both ensete fiber-reinforced polymer composites considered, the predicted in-plane Poisson ratio is observed to have a negative gradient for all analytical models and FEA, which means that as the ensete fiber volume fraction is increased, the

effective Poisson ratio decreases. From **Fig. 11 a)**, it is observed that the predicted results for the EFREC from the analytical models align and depict a linear reduction in Poisson ratio as the FVF is increased. The same is true for the EFRPC. From the two composites, the EFREC proves to have better predicted values for Poisson ratio as compared to the EFRPC. Taking reference at 0.5 fiber volume fraction, the predicted Poisson ratio value for all analytical models is 0.2625 while that of EFRPC yielded 0.2525 value for all analytical models. The FEA results for both composites also reveal the same trend as the micromechanical models in that the predicted in-plane Poisson ratio shows a decrease, though not as linear, with an increase in FVF. However, the FEA results are slightly lower than those of the micromechanical models but still within the upper and lower boundaries of the Poisson ratio values which again validates the reliability of the micromechanical models' predictions.

5.3 Strain Analysis

Depicted in **Fig. 12** through **Fig. 21** are the ANSYS structural analysis stress results for the 14 bast fiber-reinforced composites under study in this article. In this study, the RVE was assigned fixed supports on the top and bottom faces, and a compressive uni-directional load (UDL) of 10N was applied at the centre of the RVE. The results were simulated at 0.5 FVF.

5.3.1 Strain Analysis for Ensete polymer composite

Fig. 12 and **Fig. 13** show strain results for ensete and hemp fiber-reinforced polymer composites for both epoxy and polystyrene polymer matrices respectively. From the figures, there is an observed trend for both composites that higher strain occurs on the peripheral edges of the composites, as indicated by the red-orange-yellow zones, indicating maximum strain. This is because the polymer matrices, epoxy and polystyrene, have lower stiffness values, making them less resistant to deformation. Contrarily, since the ensete and hemp fibers comparatively have higher elastic moduli, they can absorb the loading effect of the force applied with minimum deformation, hence marked by the blue zones on the fiber phase, indicating minimum strain.

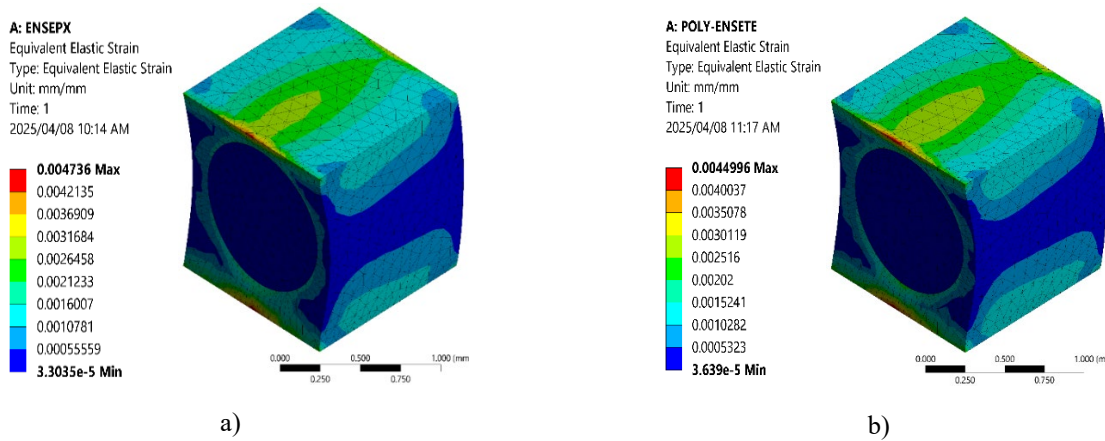


Fig. 12 Ensete strain analysis results for a) epoxy composite and b) polystyrene composite.

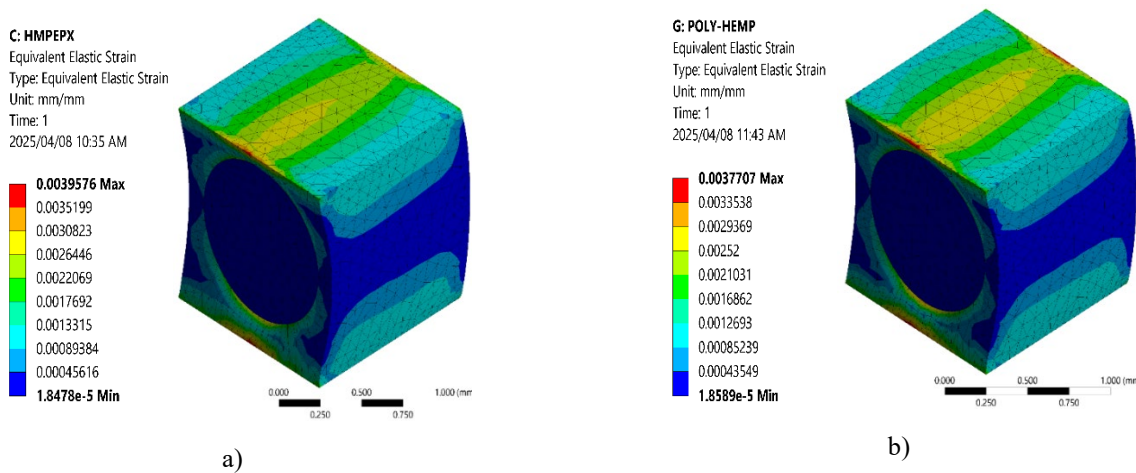


Fig. 13 Hemp strain results for a) epoxy composite and b) polystyrene composite.

Fig. 14 and **Fig. 15** show the average strain values for epoxy and polystyrene composites, respectively. It can be observed from both figures that the banana-fiber reinforced epoxy composite displayed the highest strain among all other bast fiber-epoxy composites. This is attributed to the elastic property of banana fiber. Also, the low elastic modulus of banana fiber

makes it less stiff. When used as reinforcement in a composite, it cannot be able to handle and absorb the load transferred from the matrix. This results in most of the strain being absorbed by the polymer matrix, which has relatively low stiffness and is more susceptible to deformation.

On the other hand, hemp fiber-reinforced composites show the lowest strain values for both polymer matrices, as seen from **Fig. 14** and **Fig. 15**. This is because hemp fiber has the highest elastic modulus of 70GPa and a high Poisson ratio of 0.4, making the load transfers from the matrix more effective and lateral expansion possible due to the high Poisson ratio. Comparing the strain values between the two matrix materials, an overall closeness in the strain values is observed between the two matrices, with an average difference of 2%. From this observation, it can be deduced that the two matrices could be used as an alternative to each other since they display slightly similar behavior. It is observed from the results that across all fiber-reinforced composites, there is an overall average percentage increase of about 2% in strain when transitioning from polystyrene to epoxy composites.

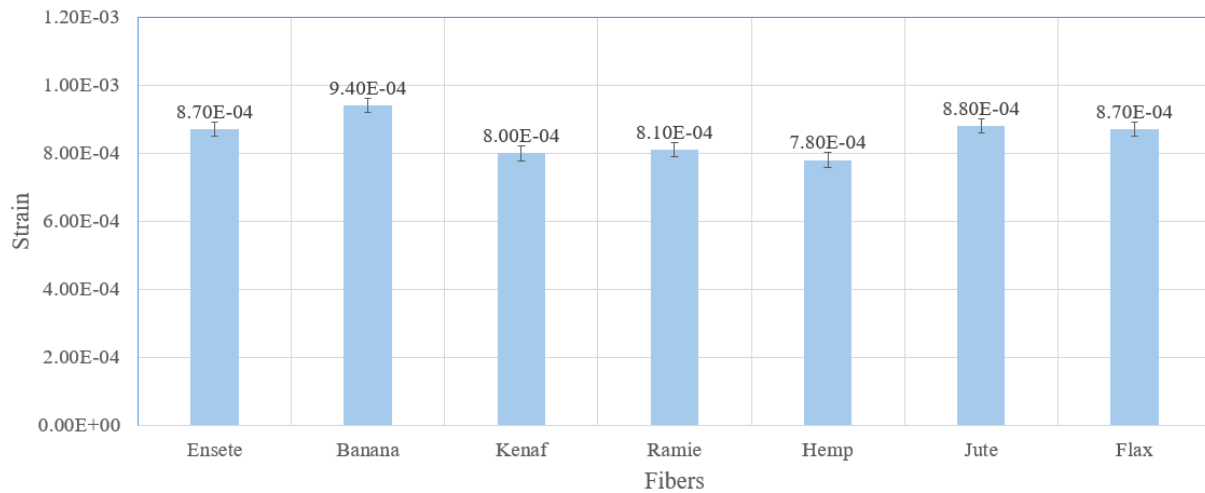


Fig. 14. Strain Analysis results with Epoxy

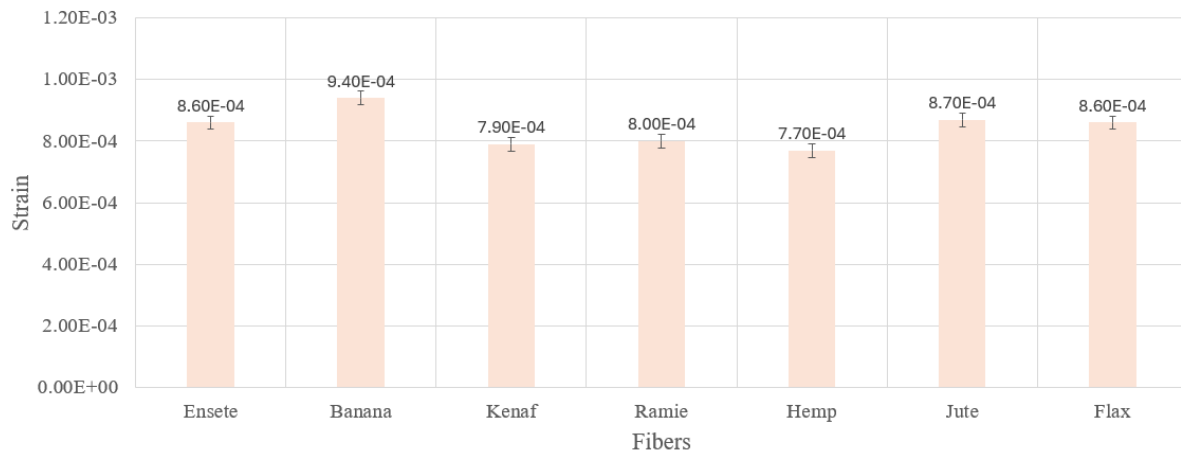


Fig. 15. Strain Analysis results with polystyrene

From both **Fig. 14** and **Fig. 15**, ensete and flax composites for both matrices show the same strain values, with 8.7×10^{-4} mm/mm for epoxy matrix, and 8.6×10^{-4} mm/mm for polystyrene matrix, respectively. It is observed, however, that ensete composites have slightly lower strain values than jute across both polymer matrices. From these comparable strain values, it can be deduced that both ensete and flax behave similarly where deformation and loading are concerned. From this, it can be suggested that ensete fiber serves as a potential reinforcement alternative for flax fiber in fiber-reinforced composites.

5.4 Stress Analysis

5.4.1 Stress Analysis for Ensete polymer composite

Fig. 16 and Fig. 17 show the equivalent (von Mises) stresses, and Fig. 18 and Fig. 19 show the average stress values for the composites. Starting with the general trend observed in the figures of ensete and hemp composites, there's a constant stress pattern of maximum stresses occurring inside the fiber and at the fixed supports, as depicted by the yellow, red, and orange colours.

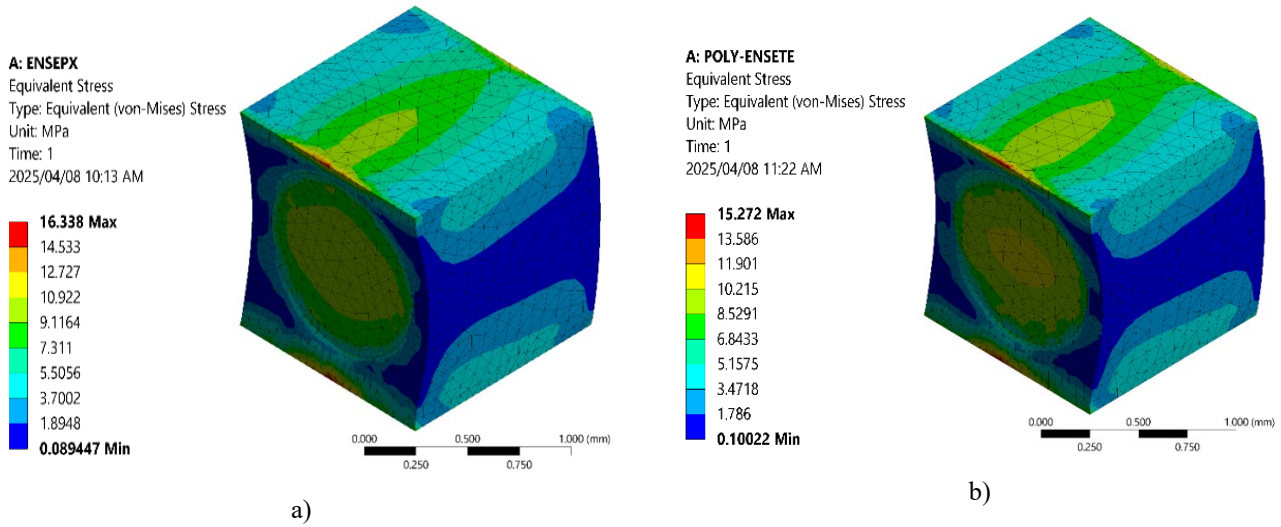


Fig. 16: Ensete stress results for a) epoxy composite and b) polystyrene composite.

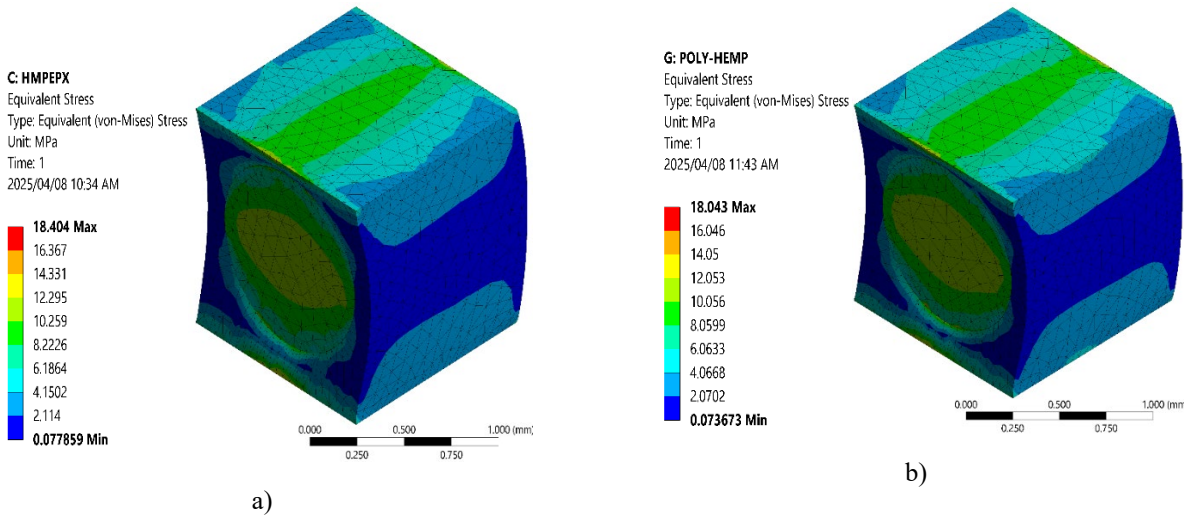


Fig. 17. Hemp stress results for a) epoxy composite and b) polystyrene composite.

For matrix comparison using Fig. 18 and Fig. 19 generally, polystyrene composites and epoxy composites using the same fiber exhibit almost the same average stress. For example, the Epoxy-banana has 5.71 MPa average stress, and the polystyrene-banana is also 5.79MPa. The rest of the fibers follow the same trend. This shows that polystyrene is comparable to epoxy as a matrix material and can, therefore, be used as a substitute. Epoxy is widely used and adopted as a matrix for composites, and introducing a new comparable material ensures variety for material design.

The slight differences in the values between epoxy and polystyrene composites stresses are because of the difference (albeit not much) in the stiffness's of the matrices. Epoxy has a higher stiffness at 3.45GPa whereas polystyrene is close at 3.4GPa. Comparing the fibers, it is noted that the average stresses have a very small range, with the lowest (banana) at 5.71MPa and the highest hemp at 6.14MPa. That is an 8% difference in epoxy. For polystyrene, it's 5.79 MPa and 6.23 MPa in banana (the lowest) and hemp (the highest) respectively, giving an 8% difference as well.

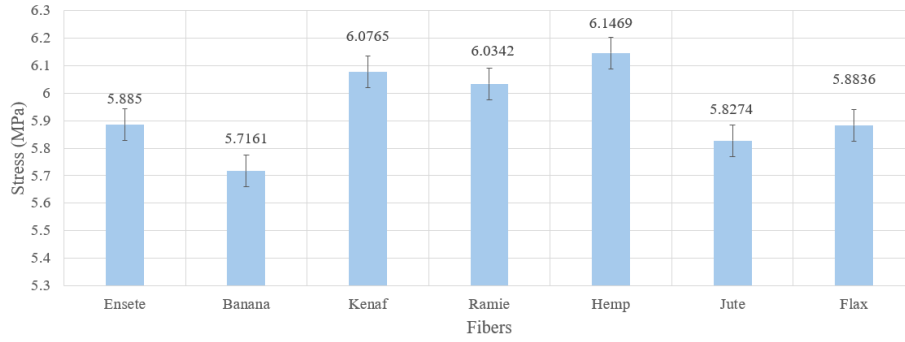


Fig. 18. Stress Analysis results with Epoxy

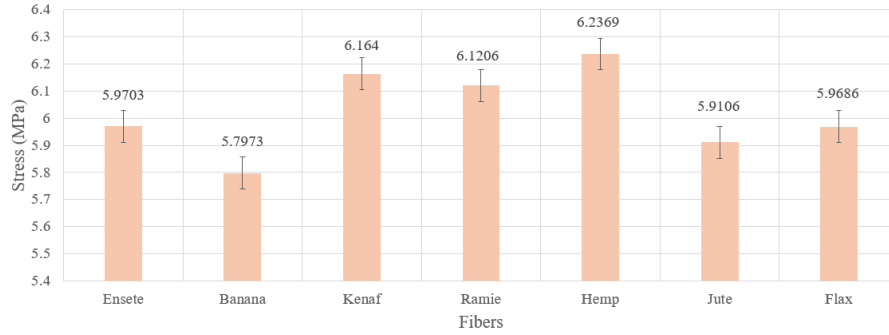


Fig. 19. Stress Analysis results with polystyrene

Looking at the maximum stress from **Fig. 20** and **Fig. 21** to further differentiate between the fibers, hemp has the highest maximum stresses of 18.4MPa in epoxy and 18MPa in polystyrene. For all fibers, the nominal (average) stress is approximately the same as already stated. However, the maximum stress is explained by the stress distribution in the composite, i.e., how the fiber and matrix share the load.

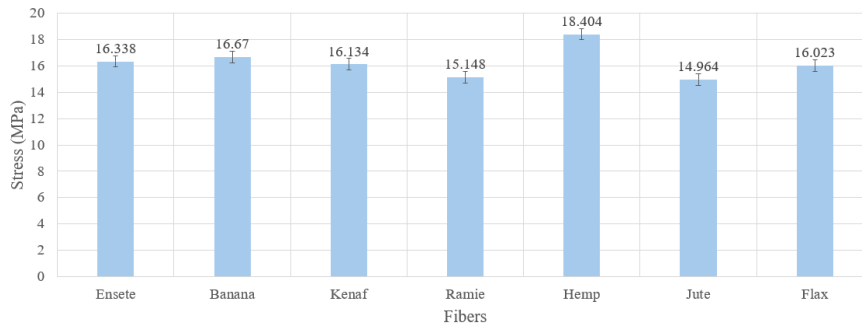


Fig. 20. Stress Analysis results (Maximum) with Epoxy

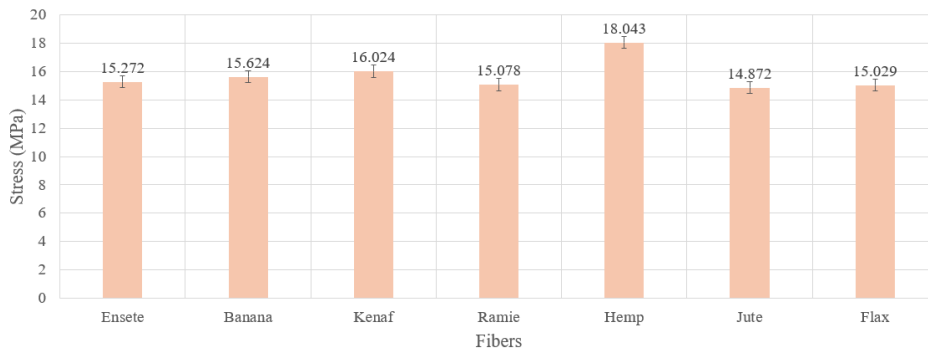


Fig. 21. Stress Analysis results (Maximum) with polystyrene

The quest to look for alternative materials and fibers is always ongoing. Therefore, the study of an unutilised material like ensete is a very welcome development. From both stress and strain sections of this discussion, it is evident that ensete has comparable characteristics to those of flax and jute. Therefore, ensete fibers can be used in composites that were originally created with jute fibers.

6. Conclusion

Based on the results and the subsequent discussion, the analysis of composite materials has shown that increasing the FVF for composites enhances and alters the elastic properties of the resulting composites. Particularly, an increase in fiber volume fraction significantly enhances composite stiffness across both epoxy and polystyrene matrices. For the first figure which depicts the Effective axial modulus E_1 of the composites against the fiber volume fraction there is a linear correlation indicating that fibers serve as effective reinforcements in the axial direction, with hemp fibers providing the highest stiffness and banana fibers the lowest. In comparison, the transverse modulus E_2 increases non-linearly, driven more by matrix properties, with epoxy yielding stiffer results than polystyrene due to its inherent rigidity. Similarly, hemp composites show superior shear modulus G_{12} with more complex models (e.g., Halpin-Tsai) capturing the mechanics of fiber-matrix bonding more accurately under shear loading. Poisson's ratio is less impacted by fiber volume and is influenced mainly by the matrix, with epoxy composites exhibiting lower Poisson's ratio than polystyrene. **Figs 8 through 11** compare FEA and micromechanical models results for EFREC and EFRPC. The results reveal that the EFREC exhibits better effective elastic properties than the EFRPC, with a very slight margin between the two. FEA results align closely with analytical models, save a bit of deviation, affirming their reliability for predicting mechanical properties. FEM results for all fibers validate the robustness of micromechanical models for analysis. In the stress-strain analysis, it is confirmed that both epoxy and polystyrene materials are good as matrix materials, and they are closer in behaviour and can thus be used interchangeably in application. Higher stresses occur in the fibers while higher strain occurs in the matrix. From **Fig. 14** and **Fig. 15** using strain rankings from highest average strain to lowest, it is banana, jute, ensete, flax, ramie, kenaf and hemp, respectively. Likewise, from **Fig. 18** and **Fig. 19** the stress rankings from highest to lowest average stresses are hemp, ramie, kenaf, ensete, flax, jute, and banana respectively.

References

- Adeniyi, A. G., Adeoye, A. S., Ighalo, J. O., & Onifade, D. V. (2021). FEA of effective elastic properties of banana fiber-reinforced polystyrene composite. *Mechanics of Advanced Materials and Structures*, 28(18), 1869-1877. <https://doi.org/10.1080/15376494.2020.1712628>
- Ahamed, B., Hasan, M., Azim, A. Y. M. A., Saifullah, A., Alimuzzaman, S., Dhakal, H. N., & Sarker, F. (2022). High performance short jute fibre preforms for thermoset composite applications. *Composites Part C: Open Access*, 9, 100318. <https://doi.org/10.1016/j.jcocom.2022.100318>
- Akil, H. M., Omar, M. F., Mazuki, A. M., Safiee, S. Z. A. M., Ishak, Z. M., & Bakar, A. A. (2011). Kenaf fiber reinforced composites: A review. *Materials & Design*, 32(8-9), 4107-4121. <https://doi.org/10.1016/j.matdes.2011.04.008>
- Ari, A., Karahan, M., Ahmed, H. A. M., Babiker, O., & Dehşet, R. M. A. (2023). A review of cellulosic natural fibers' properties and their suitability as reinforcing materials for composite panels and applications. *AATCC Journal of Research*, 10(3), 163-183. <https://doi.org/10.1177/24723444221147365>
- Arthanarieswaran, V. P., Kumaravel, A., & Kathirselvam, M. (2014). Evaluation of mechanical properties of banana and sisal fiber reinforced epoxy composites: Influence of glass fiber hybridization. *Materials & Design*, 64, 194-202. <https://doi.org/10.1016/j.matdes.2014.07.058>
- Azim, A. Y. M. A., Alimuzzaman, S., & Sarker, F. (2022). Optimizing the fabric architecture and effect of γ -radiation on the mechanical properties of jute fiber reinforced polyester composites. *ACS omega*, 7(12), 10127-10136. <https://doi.org/10.1021/acsomega.1c06241>
- Balaji, A., Purushothaman, R., Udhayasankar, R., Vijayaraj, S., & Karthikeyan, B. (2020). Study on mechanical, thermal and morphological properties of banana fiber-reinforced epoxy composites. *Journal of Bio-and Tribo-Corrosion*, 6(2), 60. <https://doi.org/10.1007/s40735-020-00357-8>
- Baley, C. (2002). Analysis of the flax fibres tensile behaviour and analysis of the tensile stiffness increase. *Composites Part A: Applied Science and Manufacturing*, 33(7), 939-948. [https://doi.org/10.1016/S1359-835X\(02\)00040-4](https://doi.org/10.1016/S1359-835X(02)00040-4)
- Batu, T., & Lemu, H. G. (2020, October). Fatigue life study of false banana/glass fiber reinforced composite for wind turbine blade application. In *International Workshop of Advanced Manufacturing and Automation* (pp. 29-40). Singapore: Springer Singapore. https://doi.org/10.1007/978-981-33-6318-2_4
- Bekele, A. E., Lemu, H. G., & Jiru, M. G. (2022). Exploration of mechanical properties of enset-sisal hybrid polymer composite. *Fibers*, 10(2), 14. <https://doi.org/10.3390/fib10020014>
- Berhanu, H., Kiflie, Z., Neiva, D., Gominho, J., Feleke, S., Yimam, A., & Pereira, H. (2018). Optimization of ethanol-alkali delignification of false banana (*Ensete ventricosum*) fibers for pulp production using response surface methodology. *Industrial Crops and Products*, 126, 426-433. <https://doi.org/10.1016/j.indcrop.2018.08.093>
- Bhambure, S. S., Rao, A. S., & Senthilkumar, T. (2023). Analysis of mechanical properties of kenaf and kapok fiber reinforced hybrid polyester composite. *Journal of Natural fibers*, 20(1), 2156964. <https://doi.org/10.1080/15440478.2022.2156964>

- Bhowmik, R., Das, S., Mallick, D., & Gautam, S. S. (2022). Predicting the elastic properties of hemp fiber—A comparative study on different polymer composite. *Materials Today: Proceedings*, 50, 2510-2514. <https://doi.org/10.1016/j.matpr.2021.09.562>
- Bos, H. L. (2004). *The potential of flax fibres as reinforcement for composite materials*. [Phd Thesis 1 (Research TU/e / Graduation TU/e), Chemical Engineering and Chemistry]. Technische Universiteit Eindhoven. <https://doi.org/10.6100/IR575360>
- Charlet, K., Eve, S., Jernot, J. P., Gomina, M., & Breard, J. (2009). Tensile deformation of a flax fiber. *Procedia Engineering*, 1(1), 233-236. <https://doi.org/10.1016/j.proeng.2009.06.055>
- Dejene, B. K. (2024). False banana (enset ventricosum) fibers: an emerging natural fiber with distinct properties, promising potentials, challenges and future prospects—A critical review. *Journal of Natural Fibers*, 21(1), 2311303. <https://doi.org/10.1080/15440478.2024.2311303>
- Dittenber, D. B., & GangaRao, H. V. (2012). Critical review of recent publications on use of natural composites in infrastructure. *Composites Part A: applied science and manufacturing*, 43(8), 1419-1429. <https://doi.org/10.1016/j.compositesa.2011.11.019>
- Djafar, Z., Renreng, I., & Jannah, M. (2021). Tensile and bending strength analysis of ramie fiber and woven ramie reinforced epoxy composite. *Journal of Natural Fibers*, 18(12), 2315-2326. <https://doi.org/10.1080/15440478.2020.1726242>
- Dunisho, F. A., Badasa, T. D., & Balasundaram, K. (2020). Improving impact strength and water absorption properties of enset fiber reinforced polyester composite. *Int J Adv Sci Res Eng*, 6(06), 138-143. <https://doi.org/10.31695/ijasre.2020.33838>
- Gholampour, A., & Ozbakkaloglu, T. (2020). A review of natural fiber composites: properties, modification and processing techniques, characterization, applications. *Journal of Materials Science*, 55(3), 829-892. <https://doi.org/10.1007/s10853-019-03990-y>
- Gupta, A., Shohel, S. M., Singh, M., & Singh, J. (2024). Study on mechanical properties of natural fiber (Jute)/synthetic fiber (Glass) reinforced polymer hybrid composite by representative volume element using finite element analysis: A numerical approach and validated by experiment. *Hybrid Advances*, 6, 100239. <https://doi.org/10.1016/j.hybadv.2024.100239>
- Júnior, C. P., De Carvalho, L. H., Fonseca, V. M., Monteiro, S. N., & d'Almeida, J. R. M. (2004). Analysis of the tensile strength of polyester/hybrid ramie-cotton fabric composites. *Polymer Testing*, 23(2), 131-135. [https://doi.org/10.1016/S0142-9418\(03\)00071-0](https://doi.org/10.1016/S0142-9418(03)00071-0)
- Ketema, S. (2021). Investigating the Mechanical Properties of False Banana Fiber Reinforced Polypropylene Composite for Panel Application (Doctoral dissertation, Bahir Dar University).
- Kiruthika, A. V. (2017). A review on physico-mechanical properties of bast fibre reinforced polymer composites. *Journal of Building Engineering*, 9, 91-99. <https://doi.org/10.1016/J.JOBE.2016.12.003>
- Mariselvam, V., & Logesh, M. (2015). Analytical analysis on material properties of kenaf fiber composite. *International Journal of Applied Engineering Research*, 10(50), 617-620.
- Malik, K., Ahmad, F., & Gunister, E. (2021). A review on the kenaf fiber reinforced thermoset composites. *Applied Composite Materials*, 28(2), 491-528. <https://doi.org/10.1007/s10443-021-09871-5>
- Malik, K., Ahmad, F., Yunus, N. A., Gunister, E., Nakato, T., Mouri, E., & Ali, S. (2022). A review of flax fiber reinforced thermoset polymer composites: thermal-physical properties, improvements and application. *Journal of Natural Fibers*, 19(15), 10412-10430. <https://doi.org/10.1080/15440478.2021.1993507>
- Mishra, T., Mandal, P., Rout, A. K., & Sahoo, D. (2022). A state-of-the-art review on potential applications of natural fiber-reinforced polymer composite filled with inorganic nanoparticle. *Composites Part C: Open Access*, 9, 100298. <https://doi.org/10.1016/j.jcomc.2022.100298>
- Müller, M., Valášek, P., & Ruggiero, A. (2017). Strength characteristics of untreated short-fibre composites from the plant ensete ventricosum. *BioResources*, 12(1), 255-269. <https://doi.org/10.15376/biores.12.1.255-269>
- Nisar, S. A., & Jamil, T. (2023). Effect of Fiber Angle on Mechanical Properties of the Natural Fiber-Reinforced Polymer Through Numerical Analysis. *Memoria Investigaciones en Ingeniería*, (25), 53-71. <https://doi.org/10.36561/ing.25.5>
- Prasad, N., Agarwal, V. K., & Sinha, S. (2016). Banana fiber reinforced low-density polyethylene composites: effect of chemical treatment and compatibilizer addition. *Iranian Polymer Journal*, 25(3), 229-241. <https://doi.org/10.1007/s13726-016-0416-x>
- Prasanthi, P., Kondapalli, S. B., Morampudi, N. K. S. R., Vallabhaneni, V. V. M., Saxena, K. K., Mohammed, K. A., ... & Buddhi, D. (2022). Elastic properties of jute fiber reinforced polymer composites with different hierarchical structures. *Materials*, 15(19), 7032. <https://doi.org/10.3390/ma15197032>
- Rao, B. L., Makode, Y., Tiwari, A., Dubey, O., Sharma, S., & Mishra, V. (2021). Review on properties of banana fiber reinforced polymer composites. *Materials Today: Proceedings*, 47, 2825-2829. <https://doi.org/10.1016/j.matpr.2021.03.558>
- Romhany, G., Karger-Kocsis, J., & Czigan, T. (2003). Tensile fracture and failure behavior of technical flax fibers. *Journal of Applied Polymer Science*, 90(13), 3638-3645. <https://doi.org/10.1002/app.13110>
- Shahzad, A. (2012). Hemp fiber and its composites—a review. *Journal of composite materials*, 46(8), 973-986. <https://doi.org/10.1177/0021998311413623>
- Shakir, M. H., & Singh, A. K. (2024). Mechanical properties, surface treatments, and applications of jute fiber reinforced composites—A review. *Polymers for Advanced Technologies*, 35(1), e6268. <https://doi.org/10.1002/pat.6268>

- Shankar, P. S., Reddy, K. T., Sekhar, V. C., & Sekhar, V. (2013). Mechanical performance and analysis of banana fiber reinforced epoxy composites. *International journal of recent Trends in Mechanical Engineering*, 1(4), 1-10.
- Singh, S. P., Dutt, A., & Hirwani, C. K. (2023). Mechanical, modal and harmonic behavior analysis of jute and hemp fiber reinforced polymer composite. *Journal of Natural Fibers*, 20(1), 2140328. <https://doi.org/10.1080/15440478.2022.2140328>
- Sivaranjana, P., & Arumugaprabu, V. J. S. A. S. (2021). A brief review on mechanical and thermal properties of banana fiber based hybrid composites. *SN Applied Sciences*, 3(2), 176. <https://doi.org/10.1007/s42452-021-04216-0>
- Sudheer, M., Pradyoth, K. R., & Somayaji, S. (2015). Analytical and numerical validation of epoxy/glass structural composites for elastic models. *American Journal of Materials Science*, 5(3C), 162-168. <https://doi.org/10.5923/c.materials.201502.32>
- Srinivas, A., Sreenivasa, C. G., & Mahadev, M. (2024, March). A review on–variants in specimen preparation of natural fiber composites. In *AIP Conference Proceedings* (Vol. 3013, No. 1, p. 020013). AIP Publishing LLC. <https://doi.org/10.1063/5.0202052>
- Srinivas, K., Naidu, A. L., & Bahubalendruni, M. R. (2017). A review on chemical and mechanical properties of natural fiber reinforced polymer composites. *International Journal of Performability Engineering*, 13(2), 189. [doi: 10.23940/ijpe.17.02.p8.189200](https://doi.org/10.23940/ijpe.17.02.p8.189200)
- Sriram, M., & Sidhaarth, K. A. (2022). Mechanical properties of ramie fibers and hooked-end steel fibers reinforced high strength concrete incorporating metakaolin and silica fume. *Journal of Building Pathology and Rehabilitation*, 7(1), 45. <https://doi.org/10.1007/s41024-022-00185-y>
- Sun, Y. M., Peng, D., & Li, M. (2011). A study of ramie fiber reinforced polypropylene composites. *Advanced Materials Research*, 194, 1839-1844. <https://doi.org/10.4028/www.scientific.net/AMR.194-196.1839>
- Teli, M. D., & Terega, J. M. (2017). Chemical, physical and thermal characterization of Ensete ventricosum plant fibre. *International Research Journal of Engineering and Technology*, 4(12), 67-75.
- Teli, M. D., & Terega, J. M. (2019). Effects of alkalization on the properties of Ensete ventricosum plant fibre. *The Journal of The Textile Institute*, 110(4), 496-507. <https://doi.org/10.1080/00405000.2018.1492321>
- Temesgen, A. G., Eren, R., & Aykut, Y. (2024). Investigation of mechanical properties of a novel green composite developed by using enset woven fabric and bioresin materials. *Polymer Bulletin*, 81(5), 4199-4219. <https://doi.org/10.1007/s00289-023-04905-3>
- Tholibon, D., Tharazi, I., Sulong, A. B., Muhamad, N., Ismial, N. F., Radzi, M. K. F. M., ... & Hui, D. (2019). Kenaf fiber composites: a review on synthetic and biodegradable polymer matrix. *J. Kejuruter*, 31(1), 65. [https://doi.org/10.17576/jkukm-2019-31\(1\)-08](https://doi.org/10.17576/jkukm-2019-31(1)-08)
- Twite-Kabamba, E., Mechraoui, A., & Rodrigue, D. (2009). Rheological properties of polypropylene/hemp fiber composites. *Polymer Composites*, 30(10), 1401-1407. <https://doi.org/10.1002/pc.20704>
- Venkateshwaran, N., & Elayaperumal, A. (2010). Banana fiber reinforced polymer composites-a review. *Journal of Reinforced Plastics and Composites*, 29(15), 2387-2396. <https://doi.org/10.1177/0731684409360578>
- Verma, N., Goyal, S., & Student, P. G. (2018). Review of Banana Fiber Composite and its Applications. *-International Journal for Scientific Research & Development*, 6 (2), 2936-2939.
- Wang, H., Memon, H., AM Hassan, E., Miah, M. S., & Ali, M. A. (2019). Effect of jute fiber modification on mechanical properties of jute fiber composite. *Materials*, 12(8), 1226. <https://doi.org/10.3390/ma12081226>
- Yan, L., Chouw, N., & Jayaraman, K. (2014). Flax fibre and its composites–A review. *Composites Part B: Engineering*, 56, 296-317. <https://doi.org/10.1016/j.compositesb.2013.08.014>
- Yusuff, I., Sarifuddin, N., & Ali, A. M. (2021). A review on kenaf fiber hybrid composites: Mechanical properties, potentials, and challenges in engineering applications. *Progress in Rubber, Plastics and Recycling Technology*, 37(1), 66-83. <https://doi.org/10.1177/1477760620953438>
- Zimniewska, M. (2022). Hemp fibre properties and processing target textile: A review. *Materials*, 15(5), 1901. <https://doi.org/10.3390/ma15051901>

